Chapter 5

INTERACTIONS WITH HSA

The data in this chapter concerning **2**, **2-Ga**, and **2-Mn** have been reproduced in part with permission from "Amphiphilic Corroles Bind Tightly to Human Serum Albumin," Mahammed, A.; Gray, H. B.; Weaver, J. J.; Sorasaenee, K.; Gross, Z., *Bioconj. Chem.* **2004**, *15*, 738. Interactions between HSA and **2-Sn** will be considered after this section.

Introduction

The bioinorganic chemistry of porphyrins is a broad field, ranging from natural to completely synthetic systems. The field also includes work on a large variety of porphyrin-like molecules (porphyrinoids), such as the chlorophyll-related chlorins and bactereochlorins as well as completely synthetic phthalocyanines and expanded porphyrins[25, 26]. A great deal of research has been devoted to the interactions of porphyrinoids with biomolecules, owing to their tendency to accumulate in cancer cells and to intercalate DNA[27, 28]. Surprisingly, although corroles have been known for almost four decades[29, 30], there has been very little work on their interactions with biological molecules. This situation does not reflect a lack of interest in these tetrapyrrolic macrocycles (they are related to the cobalt-chelating corrin in vitamin B_{12} by virtue of an identical carbon skeleton and to porphyrins by being fully conjugated), but only because

their syntheses heretofore have been long and tedious. This situation has recently changed in dramatic fashion: facile synthetic methodologies have been introduced during the last 5 years, allowing for the preparation of more than 100 new corroles[11, 14, 31-39]; transition metal complexes (Cr, Mn, Fe, Rh) of the most extensively investigated derivative (tris(pentafluorophenyl)corrole, **1**) function as versatile catalysts for a variety of organic reactions[16, 40-43]; and the Ga(III) and Al(III) complexes of corrole **1** are highly fluorescent, with quantum yields (0.37 up to 0.76) that exceed those of all other porphyrinoids[8, 44]. In addition, it has been discovered recently that electrophilic substitution of **1** offers a facile and highly selective synthetic method for the preparation of corroles with polar head groups located in only one half of the macrocycle (amphiphilic corroles)[15, 45]. This finding is key for the utilization of corroles in biological systems, since amphiphilic porphyrinoids have been shown to be the molecules of choice for many applications[46-48].

As the most abundant protein in blood plasma, human serum albumin (HSA) plays a role in many biological processes[49-51]. Available are high resolution X-ray structures of HSA as well as information about its binding affinities to many natural and synthetic molecules[52]. However, with the exception of one preliminary report, there are no X-ray structures of HSA conjugates with any porphyrinoid or related macrocyclic molecule[53]. Accordingly, information about noncovalent binding of porphyrinoids to HSA comes from data acquired by spectroscopic methods[54]. Selected results from such investigations are set out in table 5.1[55-64].

No.	Ligand[a]	Binding sites	Association constant, K (M^{-1})	Method	Ref.
1	uroporphyrin I	N=1	$(8.8 \pm 0.51)*10^4$	b	[55]
2	uroporphyrin I	N=1	$2.0*10^4$	c	[56]
3	heptacarboxylporphyrin	N=1	$(2.39 \pm 0.16)*10^5$	b	[55]
4	coproporphyrin I	N=1 another weak site	$(1.61 \pm 0.11)*10^6$ $(3.1 \pm 0.3)*10^5$	b b	[55]
5	coproporphyrin I	N=1	$(1.3 \pm 0.11)*10^5$	d	[56]
6	protoporphyrin IX	N=1	$(9.34 \pm 0.3)*10^6$	b	[55]
7	protoporphyrin IX	N=1	$0.5*10^6$	c	[57]
8	protoporphyrin IX	N=1	$1.3*10^6$	c	[56]
9	protoporphyrin IX	N=1	$2.8*10^8$	e	[58]
10	hemin	N_{strong}= 1 $N_{weak} \geq 4$	$5*10^7$ ----	f & c	[59]
11	mesoporphyrin IX		$(2.5 \pm 0.7)*10^7$	e	[60]
12	Mg-mesoporphyrin IX		$(1.7 \pm 0.5)*10^7$	e	[59]
13	Al (PcS1)	N_{strong}= 1 N_{weak}= 8	$(4.2 \pm 0.8)*10^7$ $(3.8 \pm 0.9)*10^4$	f	[61]
14	Al (PcS2) (opp)	N_{strong}= 1 N_{weak}= 8	$(2.8 \pm 1.1)*10^7$ $(4.0 \pm 0.7)*10^4$	f	[61]
15	Al (PcS2) (adj)	$N_{strong\ cooperative\ site}$= 1 N_{weak}= 8	$(5.8 \pm 0.6)*10^6$ $(2.7 \pm 0.8)*10^4$	f	[61]
16	Al (PcS3)	$N_{strong\ cooperative\ site}$ = 1 N_{weak}= 8	$(2.5 \pm 1.2)*10^6$ $(2.5 \pm 0.7)*10^4$	f	[61]
17	Al(PcS4)	nonsaturable	----	f	[61]
18	Al(PcS2)		10^4	f	[62]
19	tpss		$(5.0 \pm 2)*10^6$ $(0.2 \pm 0.1)*10^6$	f c	[63]
20	Zn(2,6-Cl, 3SO_3H)tpp	N= 7	----	f	[64]

a) Abbreviations: PcS1, PcS2, PcS3, PcS4: phthalocyanine with 1, 2, 3, and 4 sulfonato groups, respectively, where opp and adj stand for the relative positions of the sulfonato groups in PcS2 on opposite and adjacent benzopyrrole rings, respectively; tpss: 5,10,15,20-tetrakis(p-sulfonatophenyl)porphyrin; (2,6-Cl, 3-SO_3H)tpp: 5,10,15,20-tetrakis(2,6-dichloro-3-sulfonatophenyl)porphyrin. b) Affinity capillary electrophoresis. c) Fluorescence quenching of HSA by the porphyrinoid. d) Equilibrium dialysis. e) HSA-initiated changes in the fluorescence of the porphyrinoid. f) HSA-initiated changes in the absorbance of the porphyrinoid.

Table 5.1. Association constants of HSA:porphyrinoid conjugates.

In many cases, the conclusions about the number of binding sites and the association constants are based on a limited number of spectroscopic measurements, a likely reason for the significant scattering in published results that is evident from inspection of rows 6-9. Nevertheless, it is clear that only negatively charged porphyrinoids associate with HSA; and, in most cases, the protein has one well-defined high-affinity site and several other lower-affinity sites[61]. Another important finding is the inverse relationship between the association constants and the number of charged groups. The strongest association to HSA occurs with porphyrinoids that contain only two carboxylato or sulfonato groups located on the pyrrole, benzopyrrole, or phenyl rings. Intriguingly, these dipolar and amphiphilic molecules are also the most active derivatives in photodynamic therapy. A major drawback, however, is that porphyrins or phthalocyanines with a limited (<4) number of polar head groups are not readily accessible, as illustrated by the bis-sulfonated phthalocyanines that are obtained and used as a mixture of at least eight nonseparable isomers, even after separation of derivatives with a different degree of sulfonation[65].

In sharp contrast to all other synthetic porphyrinoids, the amphiphilic 2,17-bis(sulfonato)-5,10,15(trispentafluorophenyl)corrole (**2**) with its two precisely located sulfonate groups can be obtained in very simple synthetic steps from readily available starting materials[15, 45]. Accordingly, investigations of the association of **2** and its gallium(III) and manganese(III) complexes (**2-Ga**, and **2-Mn**, respectively) to HSA were performed as a first step toward utilization of corroles in bioinorganic applications. Employing several complementary physical methods, it was found that all three corroles form noncovalent conjugates with HSA. The binding affinities of these conjugates decrease according to **2** ≥

2-Ga > **2-Mn**. It is apparent that corrole **2** and its metal complexes will be fully bound to HSA under physiological conditions; accordingly, any biological activity observed for these molecules likely will be attributable to their protein conjugates.

Experimental Procedures

Chemicals. Preparations of corrole **2** and its metal complexes are described in chapter 2, and in previous publications[15, 45]. HSA was purchased from Sigma (essentially fatty acid free, catalogue no. A 1887) and used as received. Throughout these studies, 0.1 M phosphate buffer solutions of pH 7.0 were used. The extinction coefficients of the corroles under these conditions are: **2**: ε (414 nm) = 71000 $M^{-1}cm^{-1}$; **2-Ga**: ε (424 nm) = 75000 $M^{-1}cm^{-1}$; **2-Mn**: ε (422) = 21000 $M^{-1}cm^{-1}$; and for HSA, ε (280 nm) = 37400 $M^{-1}cm^{-1}$. Importantly, perfectly linear plots of O.D. vs. corrole concentration were obtained in the range of 10^{-6}-10^{-4} M, ruling out self-aggregation phenomena at the concentrations that were used in these studies. Further support for this conclusion comes from the practically identical extinction coefficients measured in aqueous and polar organic solvents (CH_3CN, MeOH).

Electronic Spectroscopy. UV-vis absorption measurements were performed on a HP8452A diode array spectrophotometer, using 3 mL of corrole solutions at 2-10 × 10^{-5} M and adding either μL portions of HSA solution or mg amounts of solid HSA.

Emission Spectroscopy. The fluorescence of HSA or the corroles was measured on an AB2 Luminescence Spectrometer. For titration of HSA's fluorescence, μL portions of

concentrated corrole solutions were added to 3 mL solutions of HSA wherein the absorbance at the excitation wavelength of 280 nm was less than 0.15. For titration of **2** or **2-Ga**, either μL portions of a concentrated HSA solution or mg amounts of solid HSA were added to 3 mL solutions of the corroles until no further changes in the emission intensity occurred.

Circular Dichroism Spectroscopy. CD spectra were recorded in the visible range on an Aviv model 62A DS Circular Dichroism Spectrometer using 3 mL of corrole solutions at 2-10 $\times$ 10^{-5} M and adding either μL portions of concentrated HSA solution or mg amounts of solid HSA. UV-CD spectra were recorded using an HSA concentration of 1.8 $\times$ 10^{-6} M (in a 4-mm cuvette) and 3.7 $\times$ 10^{-6} M (in a 10-mm cuvette) with varying ratios of **2-Ga**.

Results and Discussion

Binding of Corroles to HSA. Electronic spectra of corroles when treated with increasing amounts of HSA are shown in figure 5.1. For **2** and **2-Ga**, respective shifts of the Soret bands from 416 to 424 nm and from 424 to 430 nm are observed. For metal-free **2**, this effect could indicate changes in the protonation state of the inner N_4 core from triply- to doubly-protonated. The pKa for this process has been determined to be 5.2 in water[66], and it might be quite different in a more hydrophobic environment. However, this explanation is not believed to be correct: the changes in the Q-bands upon titration with HSA are very different from those observed upon NH-deprotonation of **2** in aqueous solutions[66], so the results are likely attributable to a "solvent effect" that would manifest itself in the interior of the protein. The same interpretation also accounts for the Soret shift of **2-Ga**. Spectral

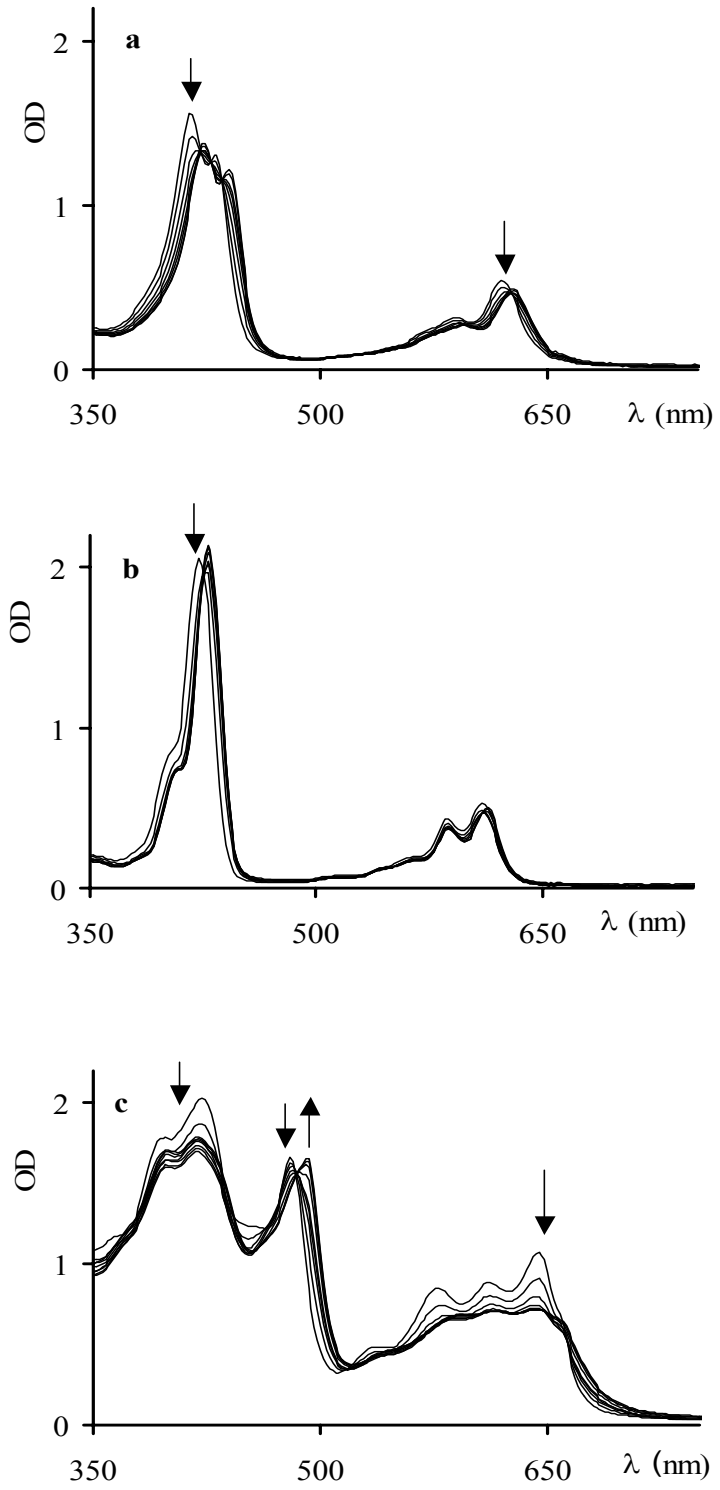

Figure 5.1. Changes in the UV-vis spectra of (a) corrole **2** and its metal complexes (b) **2-Ga**, and (c) **2-Mn**, upon titration with increasing amounts of HSA. [**2**]= 2.2×10^{-5} M, [**2-Ga**]= 2.7×10^{-5} M, [**2-Mn**]= 10^{-4} M; [HSA]= $0\text{-}10^{-4}$ M.

changes for **2-Mn** were most pronounced: most bands just decreased in intensity, but the 480 nm band was clearly replaced by a 492 nm band. It is known that this particular band (No. V in manganese(III) porphyrins) is very sensitive to axial ligation. Adding imidazole to an aqueous solution of **2-Mn** gave almost the same spectrum as addition of HSA, suggesting the participation of histidine residues in the binding of this metal complex.

In all three cases, there were no more spectral changes after the addition of about 1 equivalent of HSA, suggesting very strong association. More detailed information was obtained by following the intensity changes at selected wavelengths (figure 5.2). The majority of the intensity increase at 438 and 428 nm for **2** and **2-Ga**, respectively, is complete much before a 1:1 ratio is achieved, suggesting that there are multiple HSA binding sites for these corroles. This phenomenon is even more pronounced for **2-Mn**: the intensity at 422 nm decreases sharply up to a [HSA]:[**2-Mn**] ratio of 0.04 and increases slightly when a 1:1 ratio is approached. Taken together, the results clearly indicate that several corrole molecules associate with one protein and that redistribution takes place at higher [HSA]:[corrole] ratios in favor of the 1:1 conjugate. As the number of binding sites in protein-chromophore conjugates and the corresponding binding constants are frequently determined from Scatchard plots[67], this was also attempted with this system. However, this method and the underlying equations require the presence of unbound chromophore, while later indications show that there is no free corrole at the lowest concentrations that can be measured by UV-vis (10^{-6} M). Accordingly, none of the binding constants can be determined by UV-vis titrations.

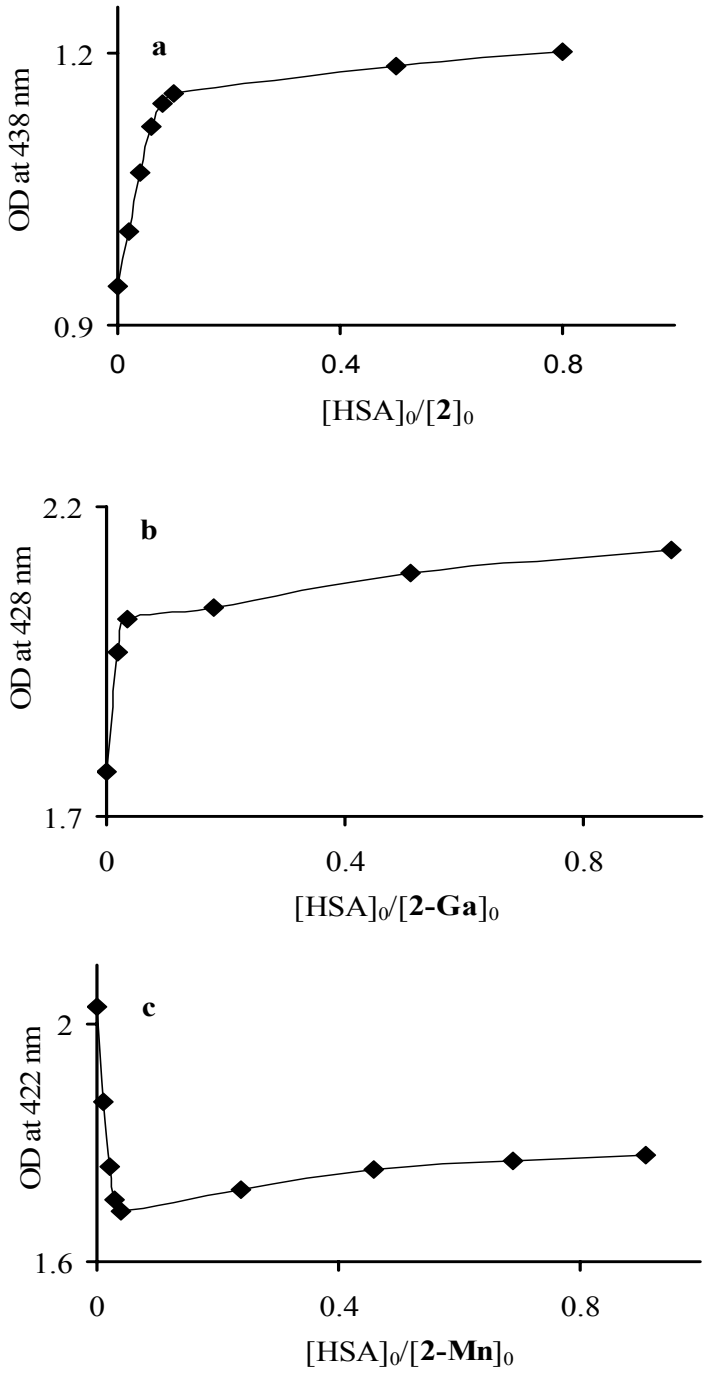

Figure 5.2. UV-vis spectral changes at selected wavelengths as a function of the [HSA]:[corrole] ratio for (a) **2**, (b) **2-Ga**, and (c) **2-Mn**.

Effect of HSA on Corrole Fluorescence. Binding of corroles to HSA can be quantified by monitoring the highly intense fluorescence of **2** and **2-Ga**, allowing experiments to be performed at significantly lower corrole concentrations. Another major advantage of fluorescence monitoring is that free and bound corroles might have different emission maxima and/or intensities. The differences in emission wavelengths of both **2** and **2-Ga** in the presence and absence of HSA are only a few nanometers, but the fluorescence intensities are very sensitive to the [HSA]:[corrole] ratio (figure 5.3). These effects are further demonstrated for selected wavelengths in figure 5.4: the initial fluorescence of **2** is reduced to less than 40 percent at a [HSA]:[**2**] ratio of 0.1:1, and it is 60 percent of the initial intensity at a 1:1 ratio. The results for **2-Ga** were even more pronounced: about 40 percent reduction at a [HSA]:[**2-Ga**] ratio of 0.1:1 and 130 percent of the initial intensity at a 1.1:1 ratio. The latter phenomenon suggests that the extent of non-radiative decay of the excited state is lowered upon binding of the fluorophore to the protein (less degrees of freedom), reflected in increased fluorescence. Nevertheless, the intensity becomes lower when many corrole molecules are bound to the same protein because of self-quenching.

For quantitative elucidation of the dissociation constants (K_d) assigned to the high-affinity binding sites, the fluorescence intensities of equimolar conjugates were measured as a function of concentration, with the expectation of a nonlinear correlation if there is significant dissociation. However, a linear correlation was obtained in the range [**2-Ga**] = [HSA] = 2×10^{-6}- 4×10^{-8} M, thereby confirming that no significant dissociation takes place, even at very low (40 nM) conjugate concentrations.

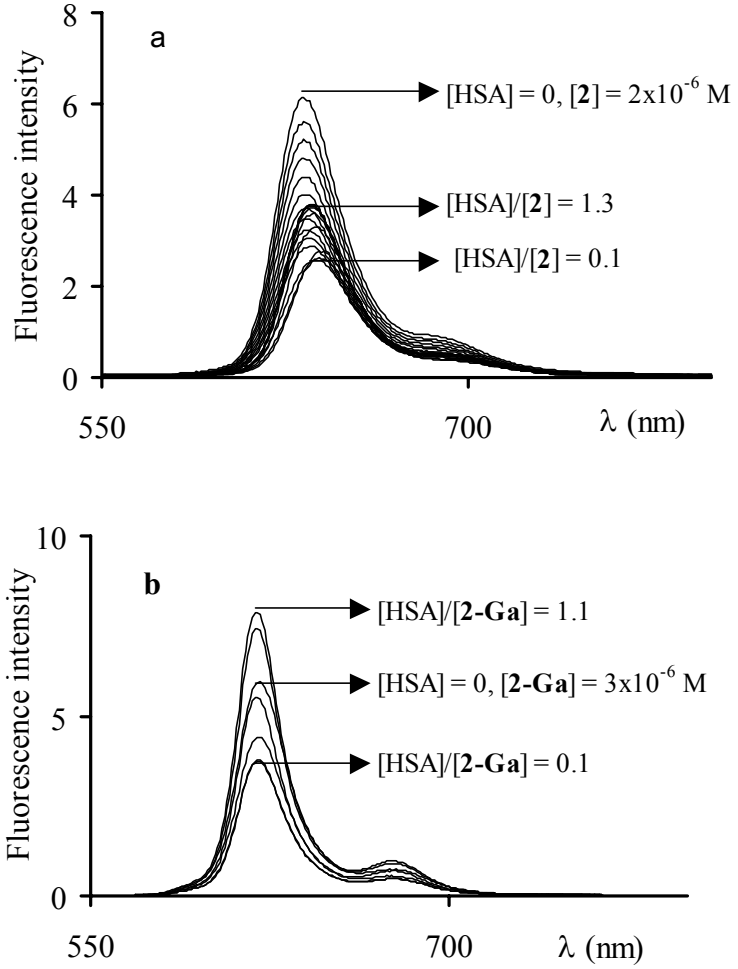

Figure 5.3. Emission spectra of corrole **2** (a, $\lambda_{exc.}$= 436 nm) and **2-Ga** (b, $\lambda_{exc.}$= 426 nm) as a function of added HSA.

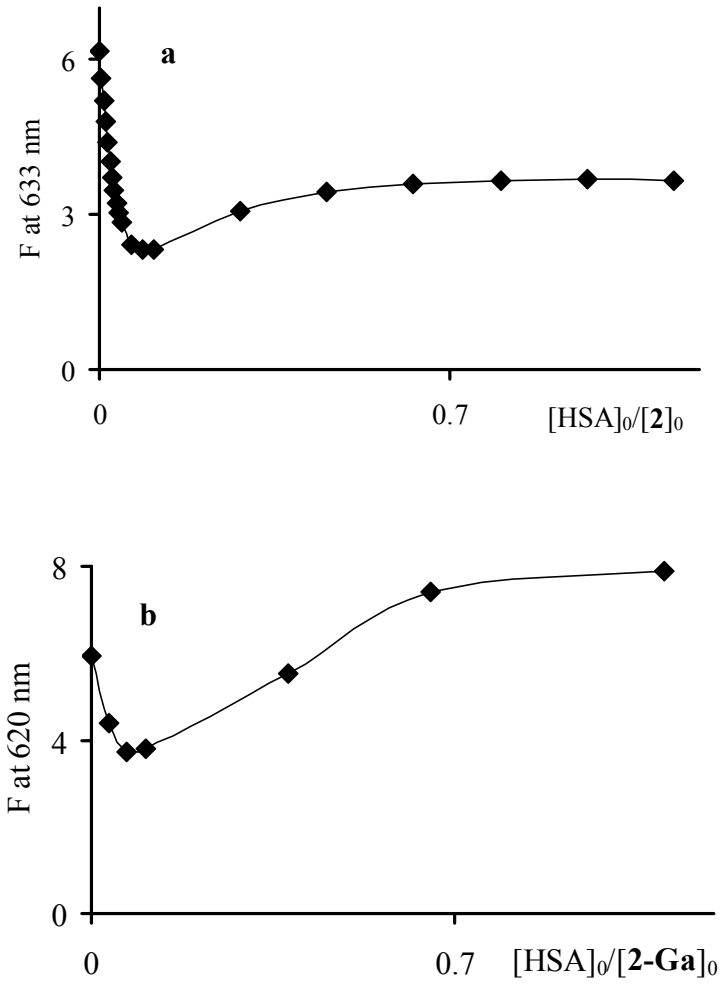

Figure 5.4. Fluorescence intensity at selected wavelengths of a) **2** and b) **2-Ga** as a function of the HSA:corrole ratio.

Circular Dichroism (CD). CD spectra of corrole solutions as a function of HSA concentration are shown in figure 5.5. Since HSA does not absorb visible light, the CD spectrum at long wavelengths ($\lambda > 360$ nm) can only be attributed to corrole interactions with the chiral environment of the folded protein. Intriguingly, the **2-Mn** CD signal (figure 5.5c) is centered at around 490 nm, which is the region of the spectrum that is most sensitive to axial ligands. Moreover, the response to HSA addition is irregular, as can be seen from the shifts of λ_{max} and the inversion from negative to positive ellipticity at 482 nm. This phenomenon is amplified at 440 and 425 nm, respectively, in the spectra of **2** and **2-Ga** (figure 5.5a-b). These data accord with the earlier conclusions about weak and strong binding sites, which in the present case is observed by redistribution of weakly bound corroles (under the conditions of [corrole] >> [HSA]) as the [corrole]:[HSA] ratio approaches 1:1. The results show that there are multiple chiral binding sites, albeit with significant differences in wavelengths and ellipticities.

CD spectra of HSA in the region 200-250 nm as a function of added **2-Ga** were also obtained to monitor possible changes of protein secondary structure in response to corrole binding[68]. As can be seen in figure 5.6, HSA gives rise to a strong CD signal at 222 nm, attributable to α-helical structures. The intensity of the signal drops as a function of the [**2-Ga**]:[HSA] ratio (0.4%, 1.1%, , 1.5%, 2% at 1:1, 2:1, 3:1, and 4:1, respectively); and, at a ratio of 10:1, roughly 8 percent of helical structure is lost. Although there is some degree of conformational change, these corrole-induced perturbations of protein secondary structure are smaller than those observed for BSA-porphyrin conjugates[67].

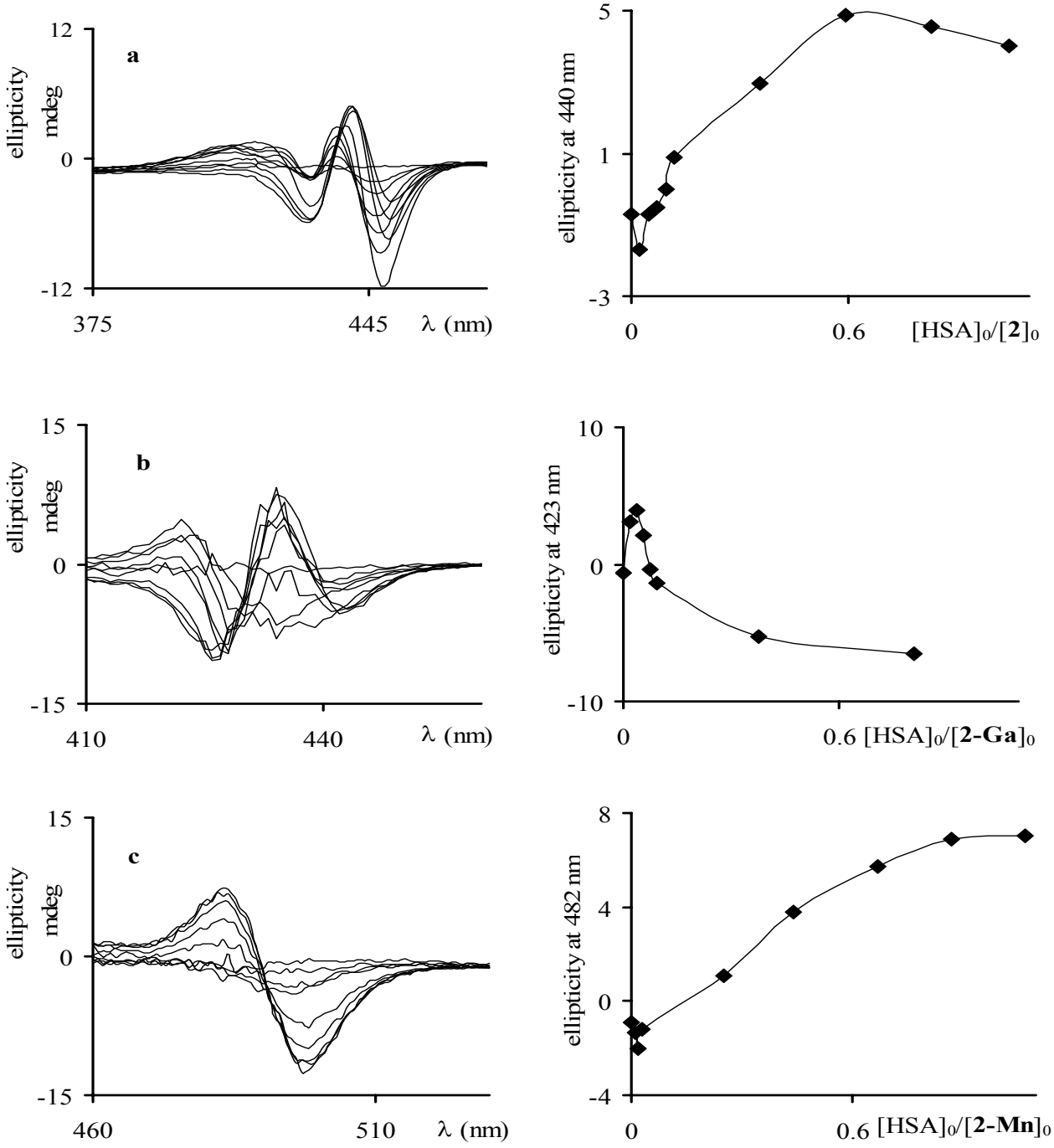

Figure 5.5. HSA titrations of (a) **2**, (b) **2-Ga**, and (c) **2-Mn**, followed by CD spectroscopy. [**2**]= 2.11×10^{-5} M, [**2-Ga**]= 2.7×10^{-5} M, [**2-Mn**]= 10^{-4} M; [HSA]= 0-10^{-4} M.

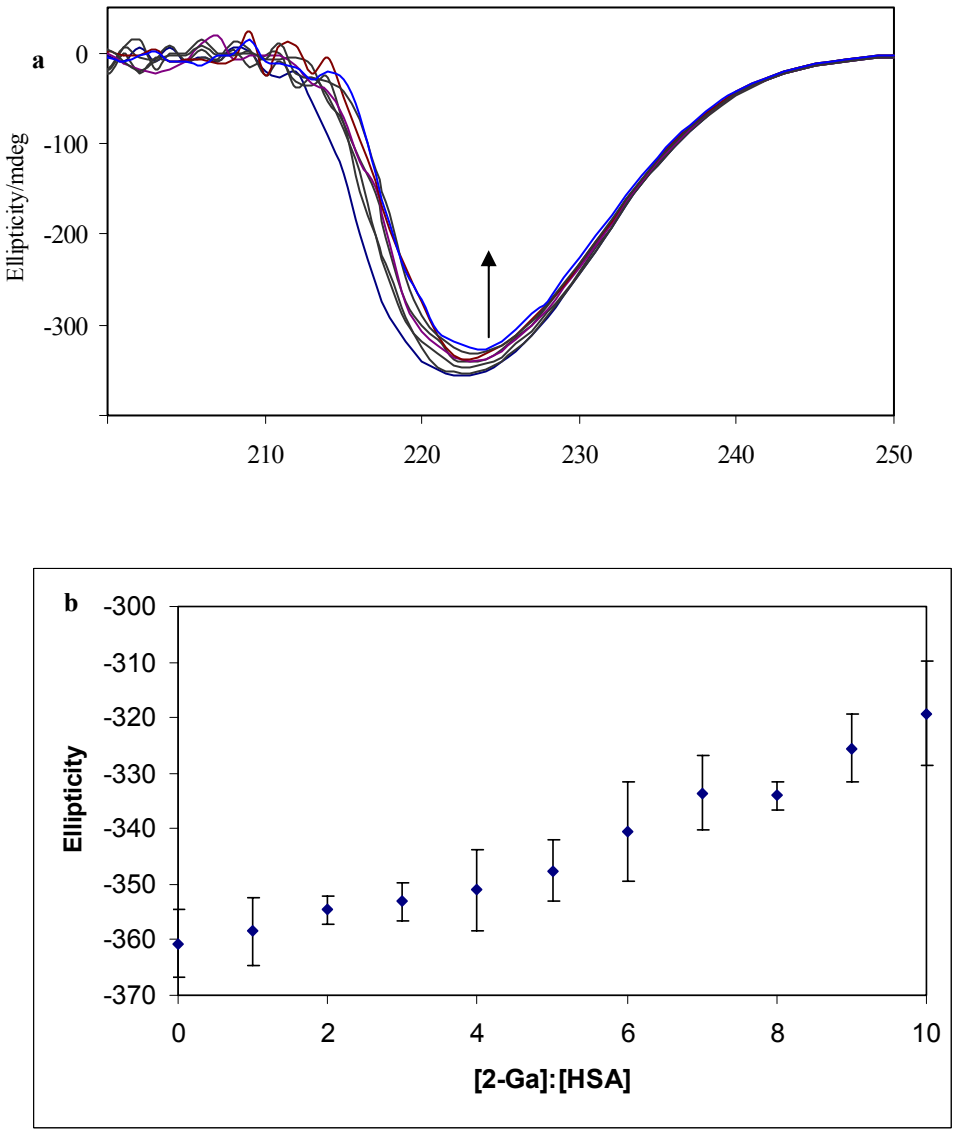

Figure 5.6. a) CD spectra of HSA as a function of [**2-Ga**]:[HSA] (0,1,2...10) at constant [HSA] (3.7×10^{-6} M). b) Ellipticity at 222 nm as a function of [**2-Ga**]:[HSA].

Quenching of Trp^{214} Emission. One of the earliest and simplest methods that was used for investigating hemin binding is fluorescence quenching of the single tryptophan residue (Trp^{214}) in HSA[59]. The advantage of this approach is that it reports selectively on binding sites that are not too distant from the fluorophore. Results obtained by exciting HSA's Trp^{214} at 280 nm and recording its emission (λ_{max} = 340 nm) as a function of the concentration of **2-Ga** are shown in figure 5.7a. Notably, full and selective quenching was achieved, as can be seen from the residual emission (λ_{max} = 310 nm) due to the many tyrosine residues that are present in HSA. More quantitative information was obtained from plots of fluorescence intensity as a function of the [HSA]:[corrole] ratio (figure 5.7b). The responses (slopes) of **2** and **2-Ga** are practically identical, and that of **2-Mn** somewhat smaller. The up to 50% quenching at equimolar concentrations of HSA and corrole obtained in the first two cases implies that **2** and **2-Ga** occupy close to Trp^{214} binding sites with very high-affinity. If **2-Mn** also associates to similar binding sites, figure 5.7b may be analyzed as reflecting an opposite relationship between the steepness of the slopes and the K_d of the HSA:corrole conjugates. This would lead to relative K_d from high-affinity sites in the order of **2** ~ **2-Ga** < **2-Mn**.

The roughly 50% quenching at a 1:1 ratio between HSA and **2** or **2-Ga** may be interpreted either one of two limiting ways: 100% quenching efficiency by sites that are only 50% occupied (= large K_d) or 50% quenching efficiency by sites that are 100% occupied (= small K_d). Two sets of experiments were performed to distinguish between these possibilities. The first consisted of dilution experiments on 1:1 mixtures of HSA and the corroles. For all three corroles (data for **2-Ga** is shown in the inset of figure 5.8) there was

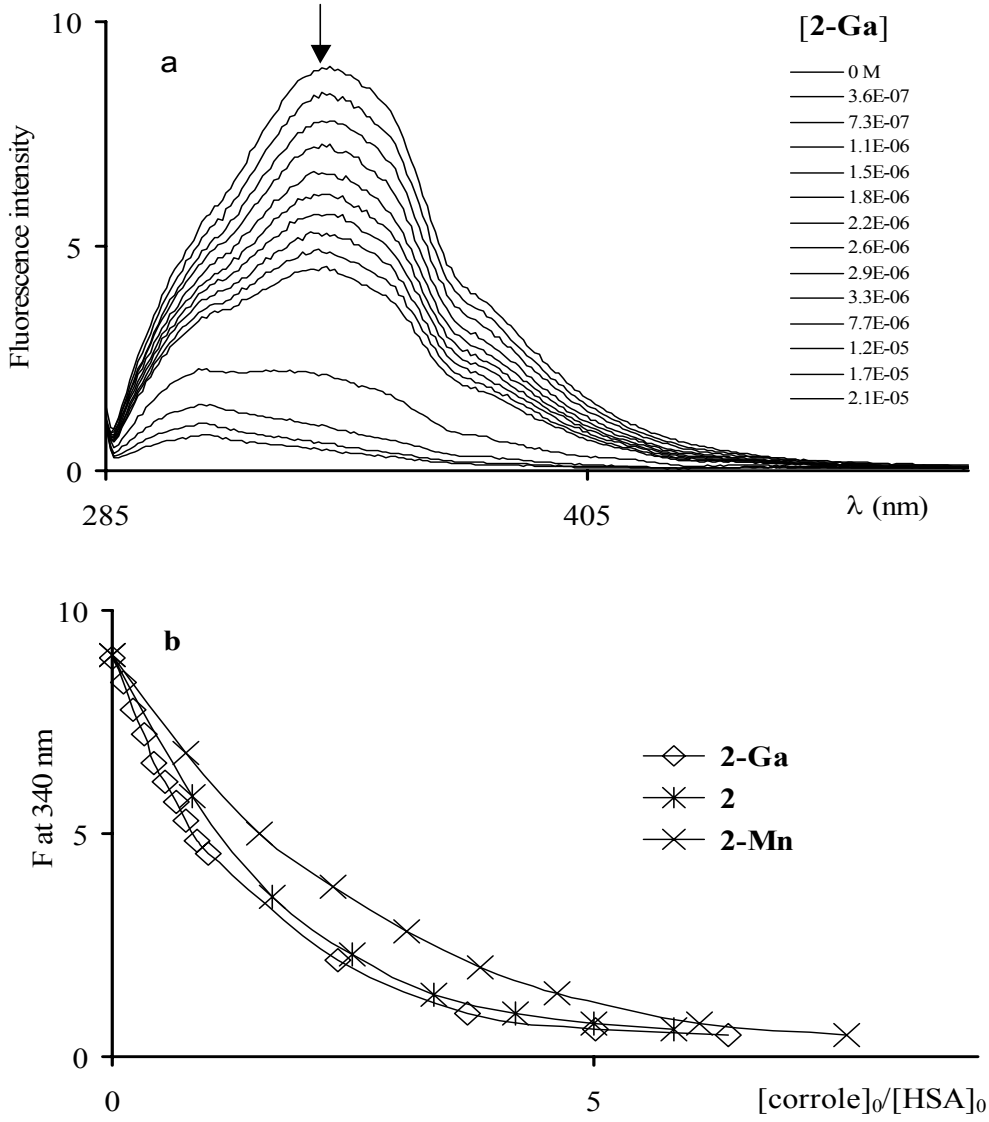

Figure 5.7. Quenching of the emission of HSA by (a) increasing amounts of **2-Ga** and (b) the dependence of the emission on the [corrole]/[HSA] ratio. $\lambda_{exc.}$= 280 nm, [HSA]= 3.3×10^{-6} M.

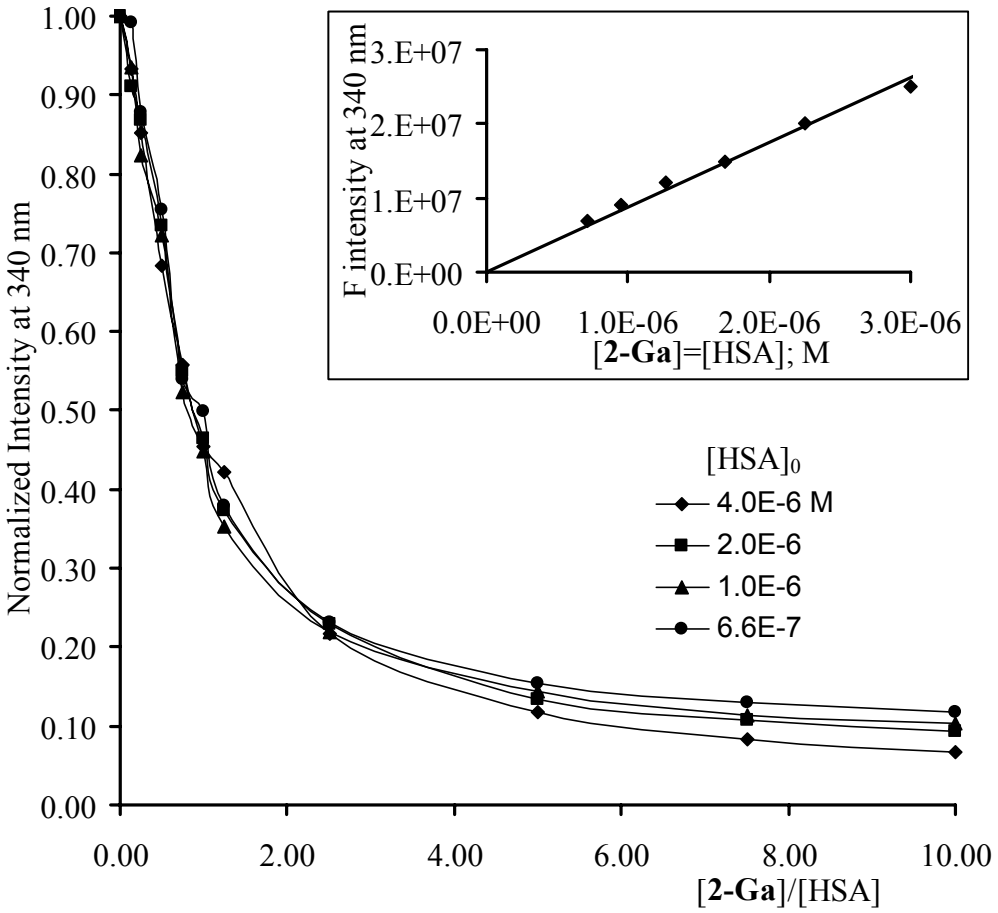

Figure 5.8. Normalized fluorescence intensity of HSA as a function of the [**2-Ga**]:[HSA] ratio at different initial concentrations of HSA. Inset: Fluorescence intensity at 340 nm of equimolar concentrations of **2-Ga** and HSA at different absolute concentrations.

no deviation from linearity in the concentration versus fluorescence-intensity plots in the range 4×10^{-6} to 7×10^{-7} M ($K_d < 10^{-8}$ M for the conjugates). Figure 5.8 shows the other set of experiments: measuring fluorescence intensity of HSA as a function of the relative amount of **2-Ga**, at four different absolute concentrations. The normalized plots are identical as long as the corrole is not in excess of HSA, clearly confirming the absence of any dissociation. The plots become different only after the [**2-Ga**]:[HSA] is above 1, indicating the presence of slightly weaker secondary binding sites. Importantly, although a reliable measurement of K_d is problematic because of the large number of corrole molecules that can be accommodated by HSA, the trends of figure 5.8 show that dissociation from weaker binding sites is very small as well. Therefore, the approximately 50% quenching seen at a 1:1 ratio between HSA and corrole is consistent with incomplete quenching of Trp^{214} fluorescence by corroles that occupy high affinity sites.

Binding Sites for 2-Ga. Since the three-dimensional structure of HSA is known, an attempt was made to estimate the distance between Trp^{214} and a corrole binding site *via* standard Förster energy transfer equations, using the roughly 50% fluorescence quenching by **2-Ga**.

$$R_o^6 = 8.8 \times 10^{-5}(\kappa^2 n^{-4} \phi_o J) \qquad (1)$$

$$J = \frac{{}_0\int^{\infty} F_o(\lambda) E_A(\lambda)\, \lambda^4 d\lambda}{{}_0\int^{\infty} F_o(\lambda) d\lambda} \qquad (2)$$

Equations 1-2 were used for evaluation of the Förster distance[69, 70], where J is the overlap between the luminescence spectrum of the donor and the absorption spectrum of the

acceptor (weighted by λ^4), ϕ_o is the luminescence quantum yield in the absence of energy transfer, *n* is the refractive index, and κ is an orientation factor dependent on the alignment of the donor and acceptor dipoles ($\kappa^2 = 2/3$ for random alignment). According to the above expressions, the experimental data yielded a value for the overlap integral *J* between the fluorescence spectrum of the protein HSA and the absorption spectrum of the quencher **2-Ga** of 6.26×10^{14}. Based on the *J* value and Equation 1, the Förster distance (R_o) between **2-Ga** and Trp^{214} (HSA) was calculated to be 30 Å. Moreover, models of the **2-Ga**-HSA conjugate based on crystallographic data for [Ga(tpfc)(py)] (tpfc = 5,10,15-tris(pentafluorophenyl)corrolate; py = pyridine) and HSA were constructed (Structural models were built using the Accelrys DS ViewerPro 5.0 software package. The structure of **2-Ga** was obtained by addition of two sulfonate groups and removal of the axial pyridine from the published crystal structure[8]: **2-Ga** was then inserted into putative HSA binding sites (crystal structure from reference 53)). In the HSA crystal structure, a heme (Fe^{III}-protoporphyrin IX) is located in a hydrophobic pocket in sub-domain IB; and there are additional interactions involving Tyr^{161}, Ile^{142}, Tyr^{138}, His^{146}, and Lys^{190} with the heme. In one of the proposed structures, where noncovalent interactions are dominant (figure 5.9a), **2-Ga** replaces the heme in the hydrophobic cavity; at this site, the distances between **2-Ga** and Trp^{214} are 20-24 Å (from the edge of the corrole-from the metal), in fair agreement with the estimated distance based on fluorescence quenching. Figures 5.9b and 5.9c show two **2-Ga**-HSA interactions that involve metal-coordination to His. As examples, it was proposed that **2-Ga** could bind to surface-exposed His^3 and His^{105} with distances between His-bound **2-Ga** and Trp^{214} of 24-30 and 30-34 Å, respectively. It is also noted that

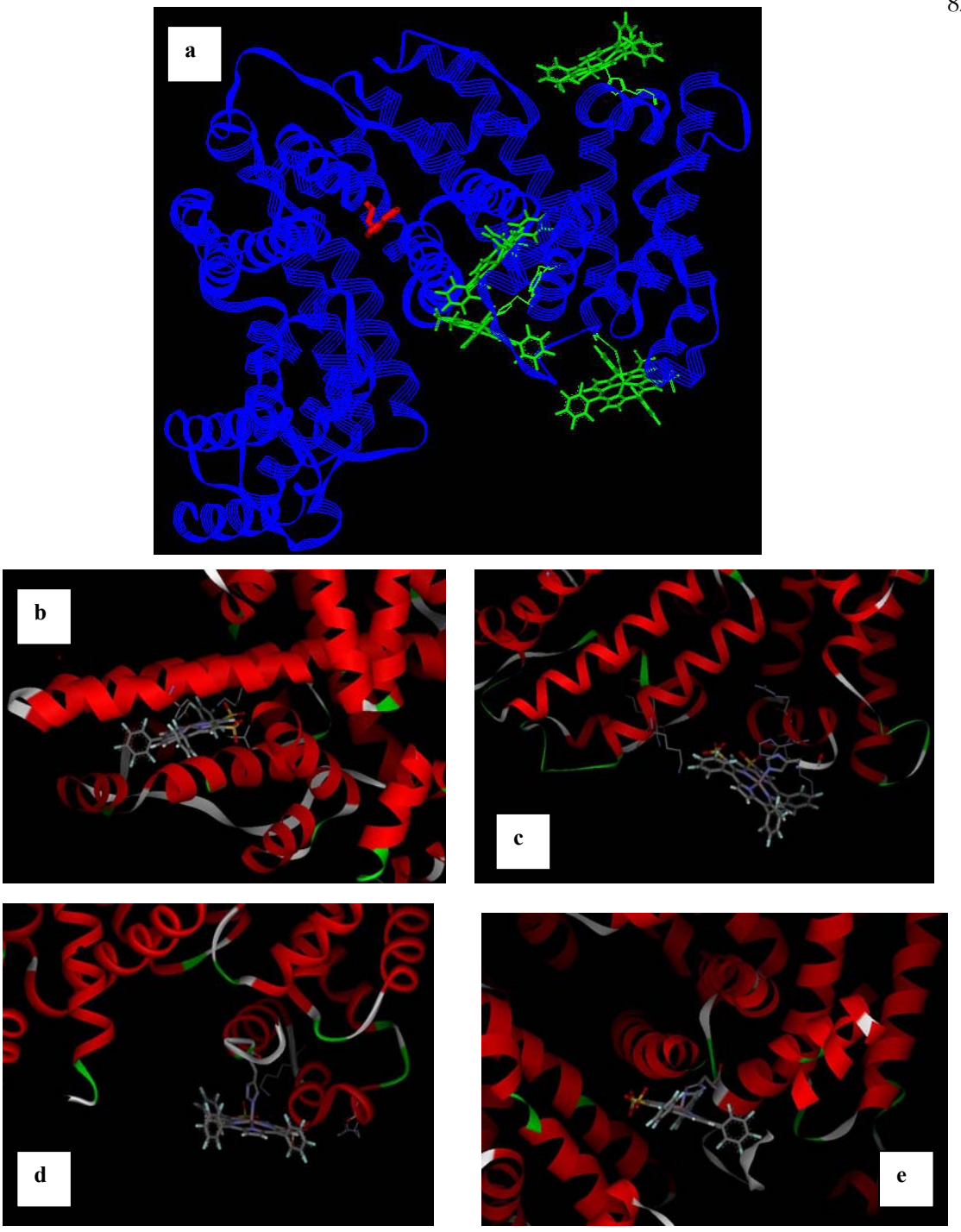

Figure 5.9. Structural models depicting four potential binding sites for **2-Ga** to HSA. (a) HSA with corroles (green) in all four potential binding sites. Trp^{214} is shown in red. (b) **2-Ga** in place of the heme of methemalbumin. (c) **2-Ga** coordinated to His^{3}. (d) **2-Ga** coordinated to His^{105}. (e) **2-Ga** coordinated to His^{146}. The proposed locations were chosen as follows: one is the heme binding site; others are histidine binding sites whose positions are consistent with the Trp^{214} quenching experiments, except for d.

coordination of **2-Ga** to His^{146} located in the heme binding pocket (figure 5.9d) is unlikely due to a considerable difference between the Förster distances measured in the model and that estimated from quenching experiments (16-19 Å vs. 30 Å).

Concluding Remarks

Reported here are results from an investigation of interactions between corroles and biomolecules. Corrole **2** is especially promising for biomedical research because of its structural similarity to the most active porphyrin-based drugs and because amphiphilicity is easily achieved. Our work has focused on interactions with HSA because any medical application must take into account associations with the most abundant protein in serum. Two metal complexes of **2** were investigated, with the goal of elucidating any effects due to ligation to relevant residues of the protein.

The changes in the electronic absorption spectra of **2**, **2-Ga**, and **2-Mn** as well as in the emission spectra of **2** and **2-Ga** as a function of increasing amounts of HSA revealed many protein binding sites. With corrole in excess, both absorption and emission intensities decreased, which is behavior that is frequently encountered when porphyrins form aggregates, usually because of limited solubility in water. However, the corroles of the current investigation do not aggregate in aqueous solutions and, accordingly, it is proposed that the above phenomena are due to self quenching of many corrole molecules that are aggregated/associated in binding pockets within the protein. Examination of published crystal structures of HSA reveals the presence of a large calixarene-like amphiphilic pocket that seems appropriate for accommodation of the corroles. When the [corrole]:[HSA] ratio

approaches 1:1, the absorption and emission intensities increase, thereby indicating redistribution of corroles from the weaker binding pocket to high-affinity sites. Many different methods were used to investigate the interactions of corroles with HSA. The results clearly show that all derivatives form tightly bound conjugates with the protein, with dissociation constants in the nM range in the order **2** ≤ **2-Ga** < **2-Mn**. Under biologically relevant conditions (HSA concentrations 2 to 3 orders of magnitude larger than those examined here) all the derivatives will be fully bound to proteins. This information is of prime importance for any potential utilization of the corroles in bioinorganic systems such as for therapeutic applications and biomimetic catalysis, approaches that are currently under investigation in the Gray and Gross laboratories.

2-Sn/HSA Interactions

2-Sn behaves much like the other sulfonated corroles when exposed to HSA. As can be seen in figure 5.10, a ~5 nm red shift is seen in the Soret bands of the corrole absorption spectrum upon HSA binding and, as with **2-Ga**, there is a slight increase in peak absorption. Note that, as with the previous corroles, the shift of the Soret band is complete before a 1:1 ratio is reached. A strong CD signal induced upon binding is also seen in figure 5.10, indicating a preferred orientation for the corrole in its binding pocket.

The fluorescence data for HSA and **2-Sn** are much like those seen with the other corroles as well. As seen in figure 5.11, the fluorescence of **2-Sn** is quenched upon binding to HSA, and the quenching levels off at [HSA]/[**2-Sn**] = 1, at approximately 20% of its initial value. Interestingly, no recovery of intensity, as in the cases of **2** and **2-Ga**, is observed.

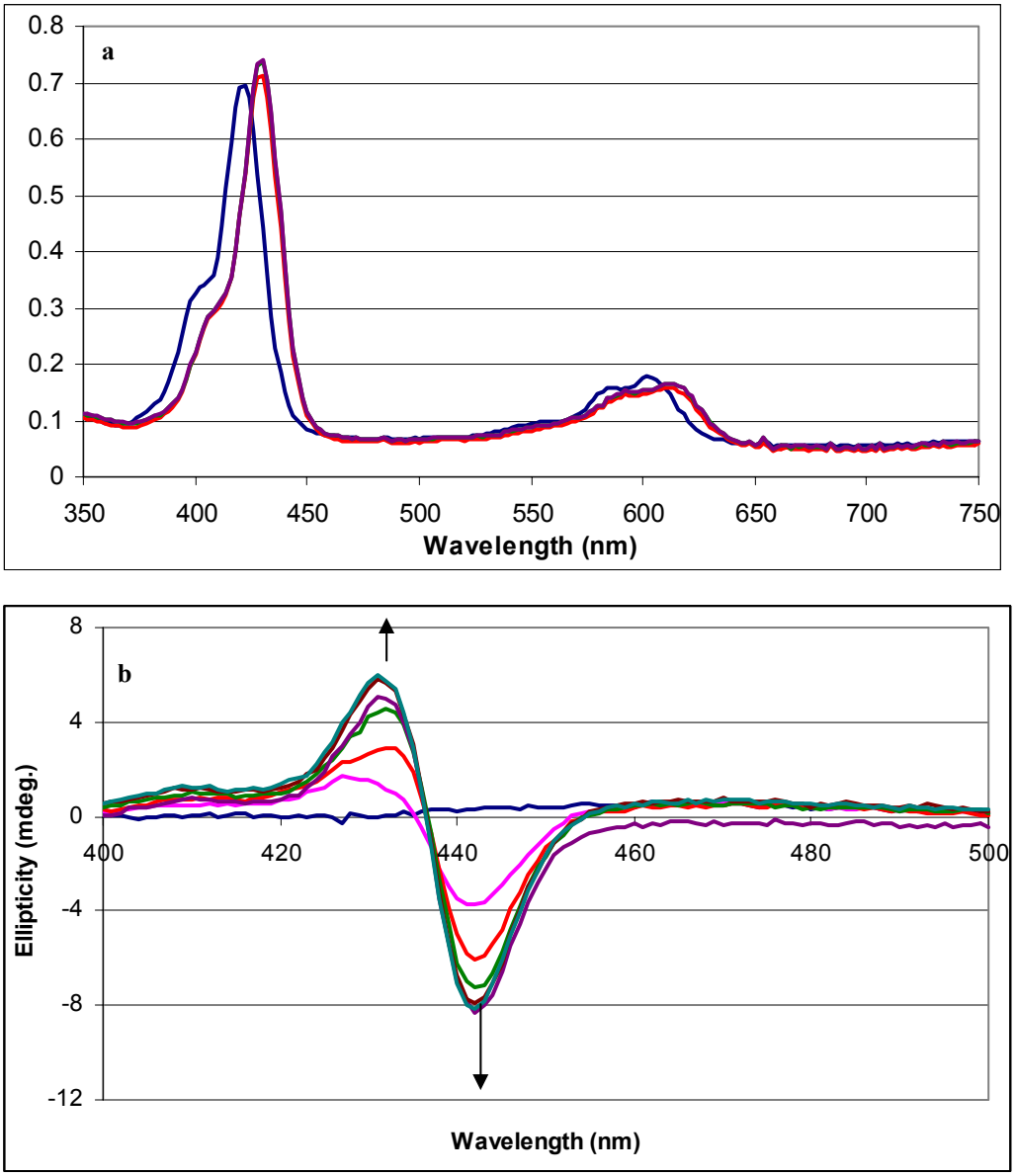

Figure 5.10. a) UV-vis spectra of HSA titrated into **2-Sn** at pH 7. [HSA]/[**2-Sn**] = 0 (blue), 0.75 (red), 1.1 (green), 1.5 (purple). b) CD spectrum of HSA titrated into **2-Sn** at pH 7. [HSA]/[**2-Sn**] = 0 (blue), 0.37 (pink), 0.75 (red), 1.1 (green), 1.5 (purple), 1.9 (brown), 2.3 (teal).

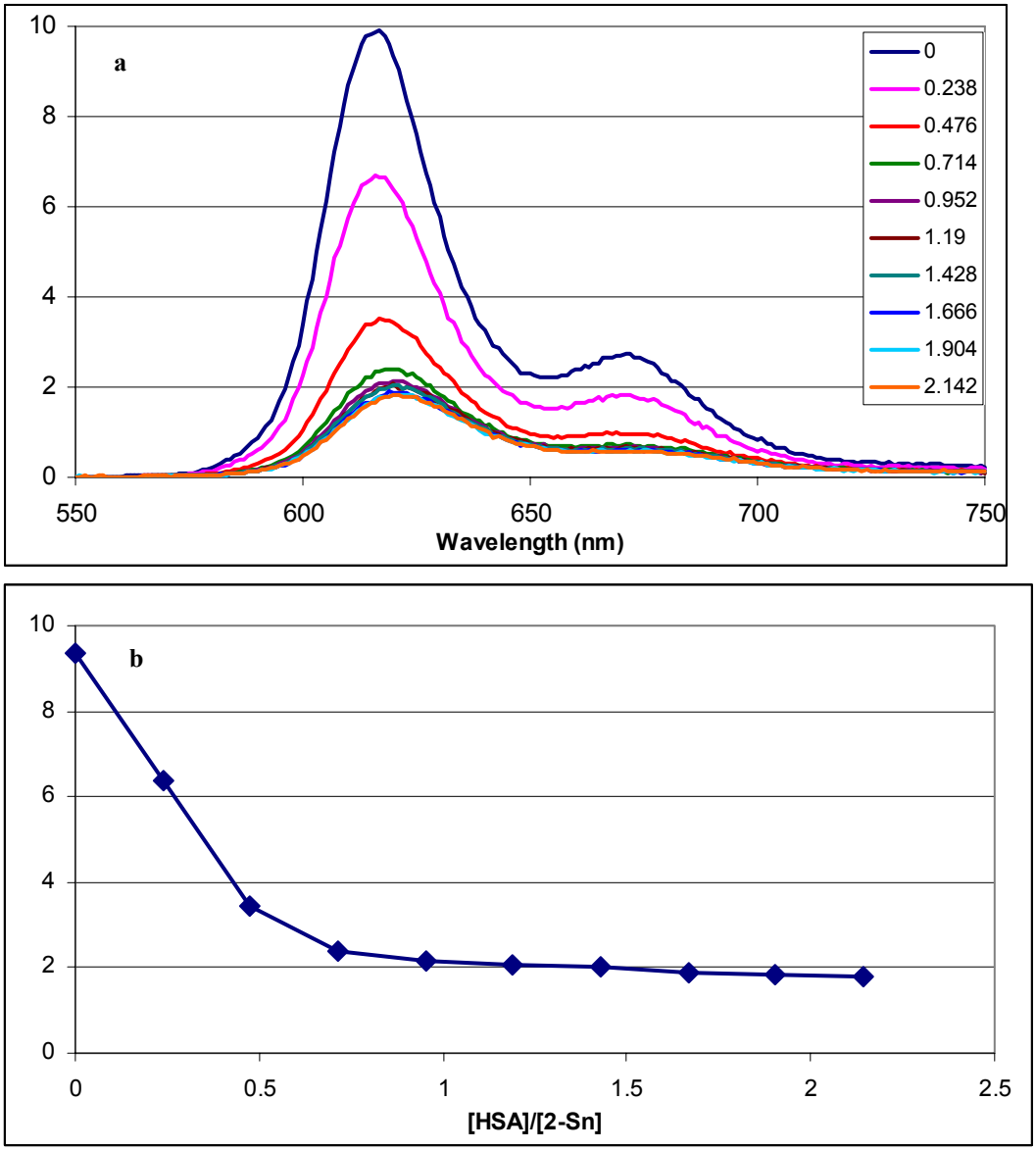

Figure 5.11. Fluorescence of **2-Sn** at varying ratios of HSA. a) Emission spectra. Ratios are given in legend. b) Peak emission versus ratio.

Studies of the tryptophan fluorescence in HSA further the similarities between **2-Sn** and the other corroles. As seen in figure 5.12, addition of **2-Sn** quenches the fluorescence of this residue, reaching ~50% quenching at a 1:1 ratio, with the amount of quenching not leveling off until [**2-Sn**]/[HSA] > 2.

2-Sn/HSA Conclusions

Studies of **2-Sn**/HSA aggregates indicate that they behave in the same manner as the other corroles studied. Thus, it seems safe to assume that the tin corrole is binding in the same manner, and likely in the same sites, as other corroles. Furthermore, the linearity of fluorescence emission for a 1:1 conjugate of **2-Sn**:HSA upon dilution indicates that the corrole binds to HSA with a similar dissociation constant, and, as with the other corroles, dissociation is undetectable by the methods used herein.

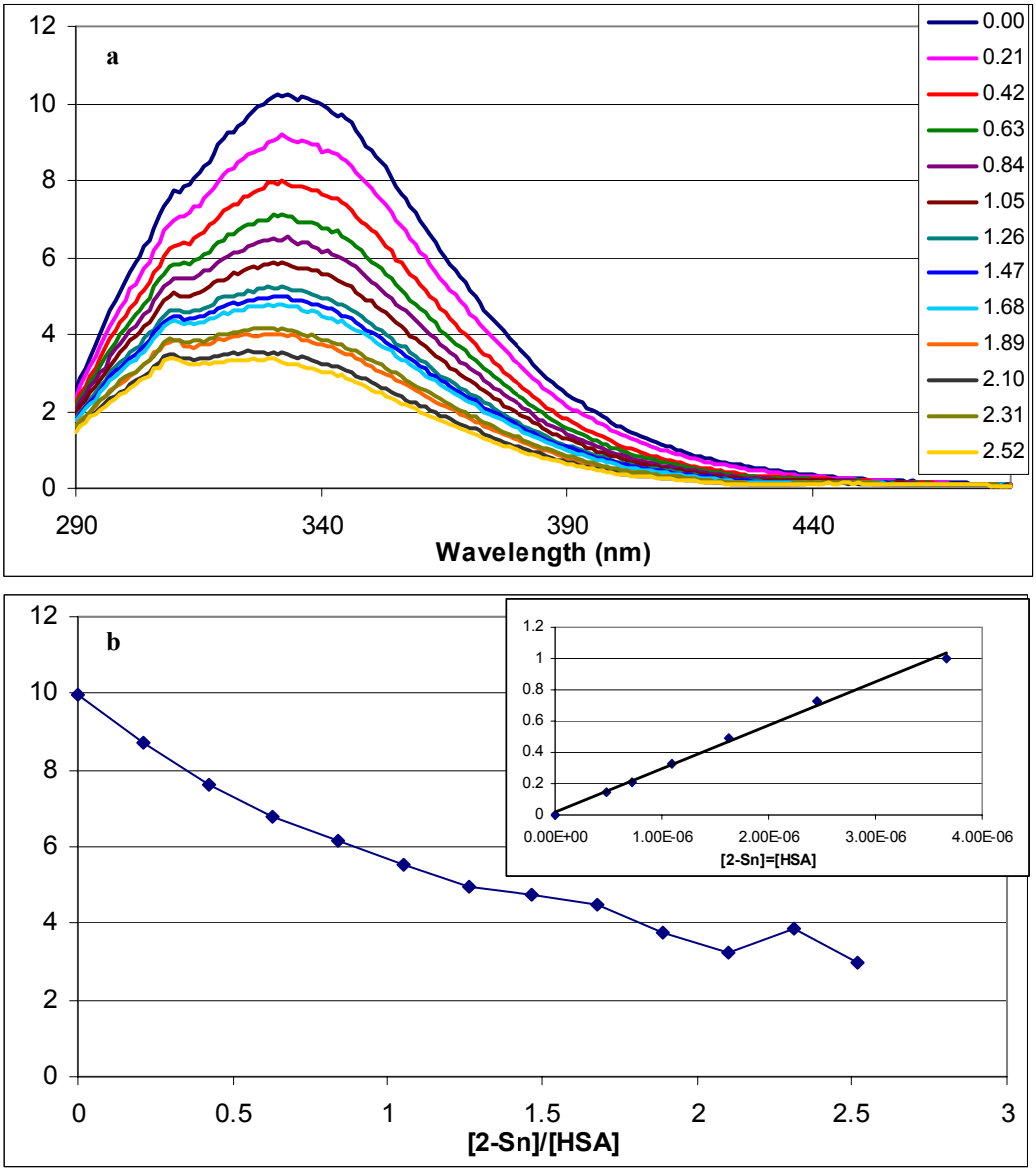

Figure 5.12. HSA tryptophan fluorescence at varying ratios of **2-Sn**. a) Emission spectra. Ratios are given in legend. b) Peak emission versus ratio. Inset shows dilution of a 1:1 mixture of HSA and **2-Sn**; concentration is given as molarity.